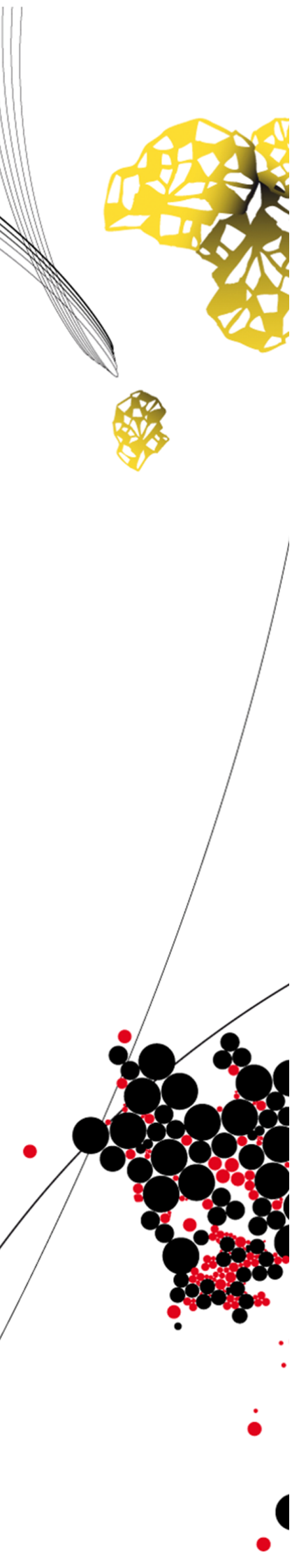

UNIVERSITY OF TWENTE.

Faculty of Electrical Engineering, Mathematics & Computer Science

Investigating the Application of Inductive Wireless Power Transfer in Real-World Drone Charging

Anand V. Nateshan

B.Sc. Thesis
June 2020

Supervisors:
prof. dr. ir. J. A. Ferriera.
prof. dr. ir. L. Spreeuwers
dr. ir. P. Venugopal

Power Electronics & Electromagnetic Compatibility Group
Faculty of Electrical Engineering
Mathematics and Computer Science
University of Twente
P.O. Box 217
7500 AE Enschede
The Netherlands

Preface

I would like to thank Dr. Venugopal for being such a helping hand during this entire thesis and for giving me interesting topics to delve into and explore to better understand my subject. Doing this really made me develop genuine interest in my research and made it a very enjoyable experience. Furthermore, I would like to extended my gratitude to Professor Spreeuwers and Professor Ferreira for their support through this process. Furthermore, my mother, father and my sister have all been pillars of support in my life and have always given me the support and confidence to do what I think is best and have complete faith in me and the decisions I make, and for that I will be forever grateful. The morals and values my mother and father have taught me from a very young age have been instrumental to my progress thus far and I am sure will continue to be key to my development as an individual. I would especially like to thank my parents for this opportunity they have given me to study something I truly am passionate about and always been there for me if ever I needed their support. My sister, Sarada, has always been the first person I go to if ever I have needed advice and has never failed to help me through difficult times. From my days in kindergarten when she would stand up for me to my days in high school were she would help me with my homework, I have been very lucky to have such an amazing sister. Lastly, I would like to thank my best friend and house mate, Joris for helping me navigate my time here in the Netherlands and for helping me make this place feel like home. For all those who have helped me along the way, Thank You, and I hope I can make you proud.

Summary

In the modern society, the automation of operations is a key driver in the progress of technologies and the ease of use of certain technologies dictates its success in wide spread adoption.

The system that is designed in this report aims to charge a 75 Watt drone in an hour and details exactly the process that is used to arrive upon the final values that are used in the system. This thesis is inspired by previous works that have looked into Wireless Power Transfer system for drones, but takes a simpler approach due to the limited amount of time given for this thesis.

The class E amplifier that drives the power transmission coils will define how the system will perform in the actual set up that will be used. Design equations by Nathan Sokal were used to craft the amplifier with the appropriate values in order to ensure zero voltage and zero current switching. A Series- Series resonant circuit is used in the amplifier as that promotes maximum current flow at the resonant frequency while minimising impedance.

Details are also presented on the receiving circuit placed on the drone as well as the specific high power MOSFET and Silicon Carbide diodes used in order to minimise losses and maximise efficiency. The size of the filter capacitor is also of importance as it smoothens out the voltage across the load to be a clean DC signal.

The design of the coils plays a major role in the overall performance of the system, and attention is paid to the different trade-offs that can be made when designing the ideal coils for a particular system. In this system, coils with high quality factors are desired as this will increase the efficiency of the system and will improve the power output capabilities. The coupling factor k also plays a role in the system and is found by looking at the self inductances of the coil and the mutual inductance. Design equations are used in order to accurately see the relationships between the different coil parameters.

The models that are used in the construction of the system are presented. A T-Model is used to simulate the power output behaviour of the circuit for certain coil inductance values at a fixed coupling coefficient. A Series- Series inductive power transfer circuit is used to see how the resonant peaks of the circuit shift when different parameters were changed, and all of these variations in the system led to

a sensitivity analysis.

The sensitivity analysis is a key way in understanding the system's behaviour when certain system parameters change. It tries to uncover how the system will react when the coupling factor changes or when the capacitance of the resonant capacitor changes and so on.

After all of the necessary steps were taken, the system is simulated together and the system is able to deliver 90 Watts of power to a battery that only requires 75 Watts to charge within an hour. It is observed that the change in the coupling factor affects the resonant frequency of the circuit quite significantly as the reflected impedance of the system changes as the coupling factor changes. Since the circuit is designed for a coupling factor of 0.2, changes in the coupling factor would result in a different reflected impedance that will move the resonant peak of the circuit.

Contents

List of acronyms

UAV Unmanned Aerial Vehicles

WPT Wireless Power Transfer

MOSFET Metal Oxide Semiconductor Field Effect Transistor

IWPT Inductive Wireless Power Transfer

List of Figures

Chapter 1

Introduction

In the coming years, we will be living in a world where drones and Unmanned Aerial Vehicles (UAV) will be a crucial part in modern society for delivery of goods, surveillance of neighbourhoods and most importantly, transportation of medical supplies from hospitals to patients or between hospitals themselves. In this future, quick and easy charging of drones and other UAV's will be of very high importance and will dictate the productivity and utility of these devices. Therefore, the infrastructure to charge these drones will be critical in the success and growth of this industry. Currently, the entire operation of charging a drone is cumbersome and time consuming as it requires a human to remove the battery from the drone, and thereafter plug the battery into the charger and then later plug the battery back into the drone. Due to this long and tedious process, the adoption of drones in delivery applications will be slow will require significant innovation in the charging infrastructure around them. By removing human interaction and making it an autonomous process, it simplifies the charging process of the drone and makes it more viable in delivery applications which require quick turn around times.

1.1 Motivation

In papers [6], [7], and [8] resonant inductive coupling have been used to create charging stations where a drone would land and immediately begin charging. However, the power output of these stations were not very high and could not supply more than a maximum of 50 W [7]. Therefore, charging speeds for a drone that is capable of carrying payloads of about 0.5 kg would be far too slow to be implementable in the real world. Furthermore, complicated alignment systems on the base station in both [6] and [7] increase costs and ease of repairability. Paper [8] described a unique idea where the drone would be fitted with a computer vision camera allowing it to track a red circle on the pad an thereby align itself with the station

during the landing process. This process requires a significant amount of components and other sensors and cameras on the drone that help it during the alignment process, and further add weight to the drone and reduce its range and payload capabilities. Therefore, this paper will focus on a simple system that consists of simply a coil in the transmitting and receiving circuit and uses resonant inductive coupling to charge the drone in a relatively short amount of time. The thesis aims to provide a refined approach to the concept of resonant inductive power transfer and aims to present a simple way to use this principle to charge a DJI F550 drone.

1.2 Research question

This paper aims to investigate the following research question:
Investigate the application of Inductive Wireless Power Transfer (IWPT) and to understand the feasibility and technical constraints of real-world drone charging:

- Analyse the impact of the coil shape and coil type on drone charging systems.
- Investigate the operation of a class E amplifier and design one that can charge a 75 Watt Drone.
- Study the impact of a Series Series and Series Parallel topology on the system performance.
- Analyse the system performance and do a Sensitivity Analysis to better understand the robustness of the system.

1.3 Report organisation

The report will follow a logical structure where first, the basic outline of the system will be laid out and all of the separate entities in the entire system will be mentioned to be further discussed in their respective chapter. Firstly, the class E amplifier used in the transmitter circuit will be divulged in Chapter 2 and its function will be analysed. In Chapter 3, the receiver circuit will be introduced and the circuit configuration and load behaviour will be analysed. Next, details will be given on the realisation of the coils in Chapter 4, and the physics and mathematics that are required to understand their function and inner workings. Later, in Chapter 5, the models will be analysed that were used to understand the functioning of the circuit. A sensitivity analysis in Chapter 6. Chapter 7 will be used to analyse the results and further propose ideas as to how the circuit could be improved in future interactions before closing out with a the conclusion in Chapter 8.

Figure 1.1: DJI F550 [1]

1.4 Drone

The drone that will be used at the model for this application can be seen in figure 1.1. The take off weight of this drone is around T_w = 3.5 kg with a payload capacity of around 0.5 kg, thus this is a drone that could potential be used in medical applications. Since it has a payload capacity of 500 grams, it could be used to transport medicine or other supplies from the hospital to a patient. The nominal battery voltage of the drone is V_{bat} = 14.4 V with a capacity of U= 4 Ah. Thus the total power required to charge the battery in an hour is 72 Watts.

1.5 Technical Introduction

The WPT system discussed in this report uses the properties of resonant inductive coupling in order to create a more dynamic and robust system. In a resonant WPT system, both the receiving and the transmitting systems are tuned to operate at a very specific frequency, which allows power to be transferred at larger distances between both two coils and allows higher power capabilities. Most modern smartphones have the capability to employ inductive coupling to charge wireless at a 5-10 Watts. This requires both the transmitting and the receiving coils to be placed right on top of each other and the system to be very well aligned. Any axial misalignment will not charge the device. However, in a resonant inductive coupling system, the tolerance for misalignment and distance between the coils is much larger and power can be transferred between the coil even if the they not axial aligned. Since both the coils are tuned to the same frequency, it creates an ”energy tunnel” which allows energy to flow between the two coils even at greater distances due to them both operating at the same frequency. The system outlined in this report operates at 13.56 MHz where both the resonant circuits are tuned to operate at that frequency.

Chapter 2

Class E Amplifier Design

2.1 Introduction

The class E amplifier used in this circuit forms the backbone of the WPT system the proper and appropriate construction of this circuit will be essential in the successful transfer of 75 Watts. There are many different amplifier topologies that exist for a myriad of different applications but, for high power transfer applications, the class E amplifier is preferred due to it being a switched-mode power amplifier. A switched-mode amplifier distinguishes itself from other amplifier as does not operate in the linear region as class A, B, A/B, C amplifiers do, but it rather operates in the sub-threshold and the saturation region, thereby eliminating losses on the MOSFET of the class E amplifier. This phenomenon will be explained in section 2.2 and forms the fundamentals principle of operation for this amplifier.

2.2 Working Principle of Class E Amplifiers

The class E amplifier falls under the category of a switched-mode amplifiers where the MOSFET is used acts as a switch and is either completely on (closed) or completely off (open) thereby preventing any losses from occurring in the MOSFET itself. In other non- switched-mode amplifiers, the MOSFET's operate in the linear region therefore burning power on the MOSFET in order to have a linear output curve. In switched-mode amplifiers, the gate source voltage is a square wave signal that either completely turns on the MOSFET with a voltage much higher than the threshold, or no voltage, thereby completely turning off the MOSFET. In this way, the MOSFET acts like a switch and no power is burned on the the active component. At the megahertz frequencies, if power was being burned on the MOSFET, the overall efficiency of the system would be negatively affected.

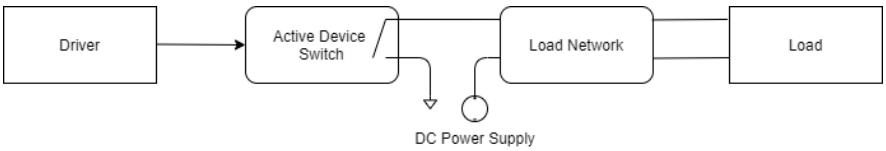

Figure 2.1: Class E Amplifier Block Diagram

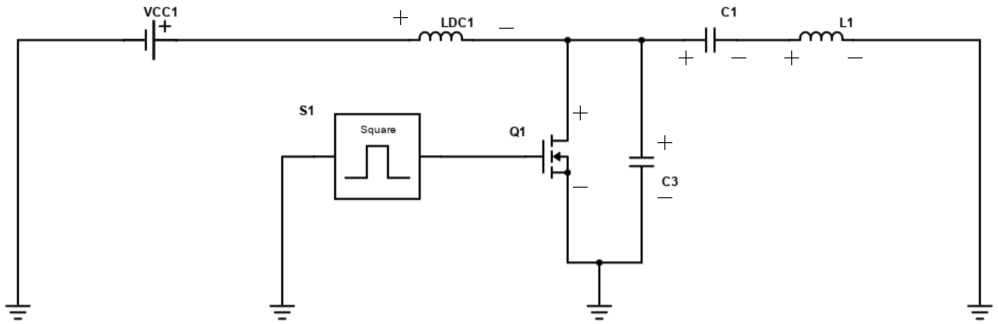

Figure 2.2: Class E Amplifier Circuit

2.3 Class E Amplifier Circuit Diagram

A block diagram of how the class E amplifier functions can be seen in figure 2.1, where the driver drives the MOSFET at the desired AC output frequency making it act as an on off switch which thereafter converts the DC signal from the power supply to the AC signal at the desired switching frequency. The input signal is a square wave at the desired output frequency and it has been seen through experimentation [9], that a duty cycle of around 50% yields the maximum fundamental frequency output. As stated earlier, to maximise the efficiency of the system zero voltage switching (ZVS) must be achieved. At turn on, there should be zero voltage across the MOSFET, while at turn off, there should be zero current across the MOSFET.

The circuit configuration used in this WPT application is highlighted through figure 2.2 and displays how all of the components of the circuit are connected to each other and how the square wave driving signal creates a sinusoidal output across inductor L_1.

2.4 Zero Voltage Switching and Zero Current Switching

In power amplifiers, the majority of the power losses occur in the active components, which is, in this case, the field effect transistor. Implementing zero voltage switching from turn off to turn on and zero current switching from turn on to turn off form the

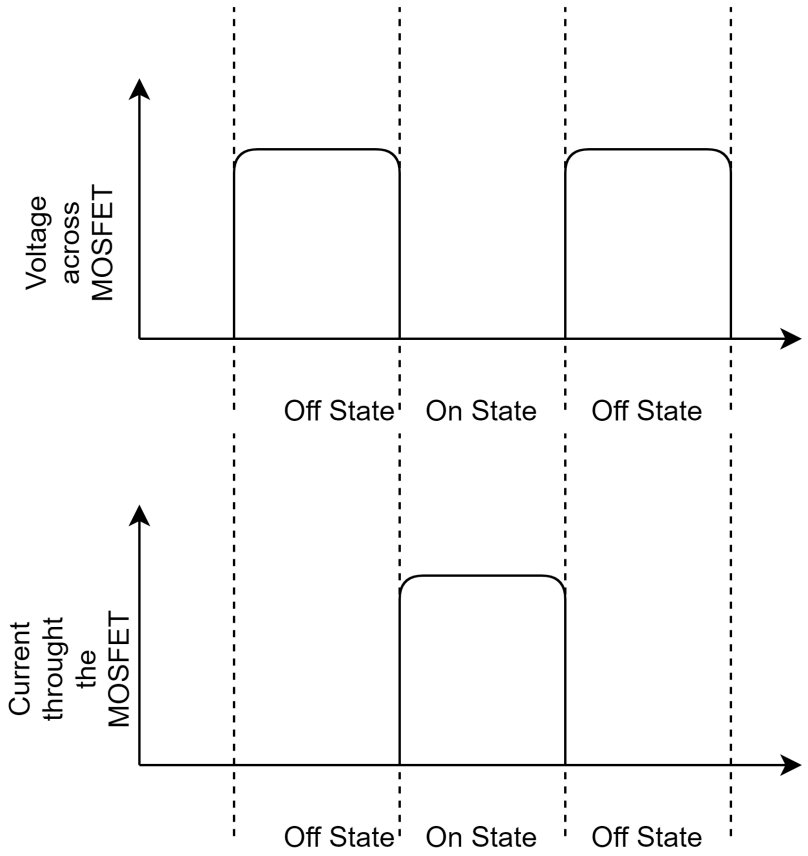

Figure 2.3: Top: Voltage across the switch when it is open and closed Bottom: Current across switch when it is open and closed

basis of switched-mode amplifiers by ensuring that when the MOSFET is turned on, there is no voltage across it and similarly, when the MOSFET is turned off, there is no current going through it. These two conditions ensure that there will be very minimal power loss on the MOSFET itself and thereby increasing the efficiency of the entire system.

To ensure that there is no voltage from turn off to turn on of the MOSFET the value of capacitor C_3 from figure 2.2 must be chosen in a way that allows it to completely discharge itself into the resonant circuit. Similarly, when going from the MOSFET on state to the off state, there should be no current going through the MOSFET which is also dependent on the component values chosen for the resonant circuit in conjunction to capacitor C_3. Since capacitor C_3 and the MOSFET are in parallel, an voltage across the capacitor would mean a voltage across the MOSFET, thus during the transition from turn on to turn off, the capacitor must be completely discharged through the switch and have zero charge on it.

This principle is shown in figure 2.3 where figure 2.3a displays the voltage across the switch with respect to time and figure 2.3b displays the current through the switch with respect to time. As can be seen, both the current and voltage through and

across the switch do not occur at the same time, thereby mitigating switching losses in the system.

2.5 Circuit Analysis

In figure 2.2, inductor L_{DC1} is used as a DC choke which blocks high frequency AC signals and only allows DC current to pass through. This is done to prevent the AC signal from the output of the transistor to go back through the inductor and into the power supply. Since the impedance of an inductor is $j\omega L$, it acts as a short of low frequencies and as an open circuit for high frequencies. C_3 is the sum of the shunt capacitance, the transistors output capacitance and the wiring capacitance. When the transistor is switched on (closed state of the switch) the voltage across it is the collector emitter voltage V_{ce} and while the transistor is switched off (open state of the switch), the transient response of the load network is that of a damped second order filter with series connections of L_1, and $\frac{C_1 \cdot C_3}{C_1+C_3}$. L_{DC1} is chosen large enough such that it can act as a source of constant current while some of the energy stored in C_1, C_3 and L_1 is delivered to R_{Load} in the secondary circuit. Since the voltage across the transistor is also the voltage across the capacitor C_3 it is very important that the capacitor C_3 is completely discharged at the switch closing time. The energy from C_3 must be dissipated into the resonant circuit to ensure no voltage across the MOSFET at time of turn on. Inductor L_1 and capacitor C_1 form the series resonant circuit. The resonant circuit in the receiver circuit is also a series resonant circuit.

Series- Series resonant circuits are being used and they work on the fundamental principle of the reactance of the capacitor cancelling out the reactance of the inductor at the resonant frequency of the system. The reactance of an inductor can be described using equation 2.1 and the reactance of a capacitor is described using equation 2.2. When $X_L > X_C$ the circuit is inductive and when $X_C > X_L$ the circuit is considered capacitive [10]. As these two equations [10] highlight, the reactance of an inductor scales proportionally with frequency and the reactance of a capacitor scales inversely with frequency.

$$X_L = 2\pi f L = \omega L \tag{2.1}$$

$$X_C = \frac{1}{2\pi f C} \tag{2.2}$$

If the system is below the resonant frequency, it is considered to be a capacitive circuit, which means that more energy will be lost in the capacitor (more impedance). When the system is above the tuned resonant frequency, the system is considered inductive, where the inductor will have contribute to more system impedance and

will not cancel out with the impedance of the capacitor. At the moment when the inductive and the capacitive reactances are equal to each other, the circuit is then in its resonant frequency, which is where the impedance of the circuit is at its minimum. Since the two reactances cancel each other out, the LC combination acts as a short circuit. Therefore, at the resonant frequency, there is maximum circuit current as the only resistance present in the circuit is the parasitic resistances of the components. The Q factor in a series resonant circuit is dictated by the relationship between the resistance, inductance and the capacitance of the circuit as shown in equation 2.3 [10]

$$Q = \frac{1}{R}\sqrt{\frac{L}{C}} \tag{2.3}$$

A parallel resonant topology could have also been chosen to be implemented in the WPT circuit but there were some key pitfalls of the parallel resonant circuit that made it less suitable for this use case. At the resonant frequency, which is determined in the same manner as the series resonant circuit, the circuit has maximum impedance, which means that the current is at the minimum. The applications of a parallel resonant circuit is very different as the resonant frequency, it rejects the current flow.

2.5.1 MOSFET Conducting State

In figure 2.4 there are two plots visible, the blue one which is the square wave driving the MOSFET and the black plot which is the voltage across the MOSFET as the switch (MOSFET) is open and closed. As seen, when the switch is open, there is a voltage peak that builds up on the switch (Capacitor C_3) and once the switch is closed, the voltage decrease to zero. By having this behaviour in the circuit, it ensures that no power is dissipated during the conducting state of the switch.

The current behaviour of the entire system can be seen in figure 2.5. In the figure, all of the relevant currents are plotted to understand how the current flows in the circuit. The blue, black and red curves are the current going into inductor L_1, capacitor C_3 and the MOSFET respectively. The purple curve is the driver of the MOSFET and the turquoise curve is the current coming out of inductor L_{DC1}. Starting from the left of the graph, when the MOSFET is conducting, allowing current to flow to ground, the current through the MOSFET increases as can be seen from the rising red curve. At the same time, the current going into inductor L_1 goes negative, meaning current is coming out of L_1 and going into the MOSFET. As the current through the MOSFET increases, the current going into inductor L_1 decreases and switches polarity and current starts flowing out of the inductor at the same rate as current

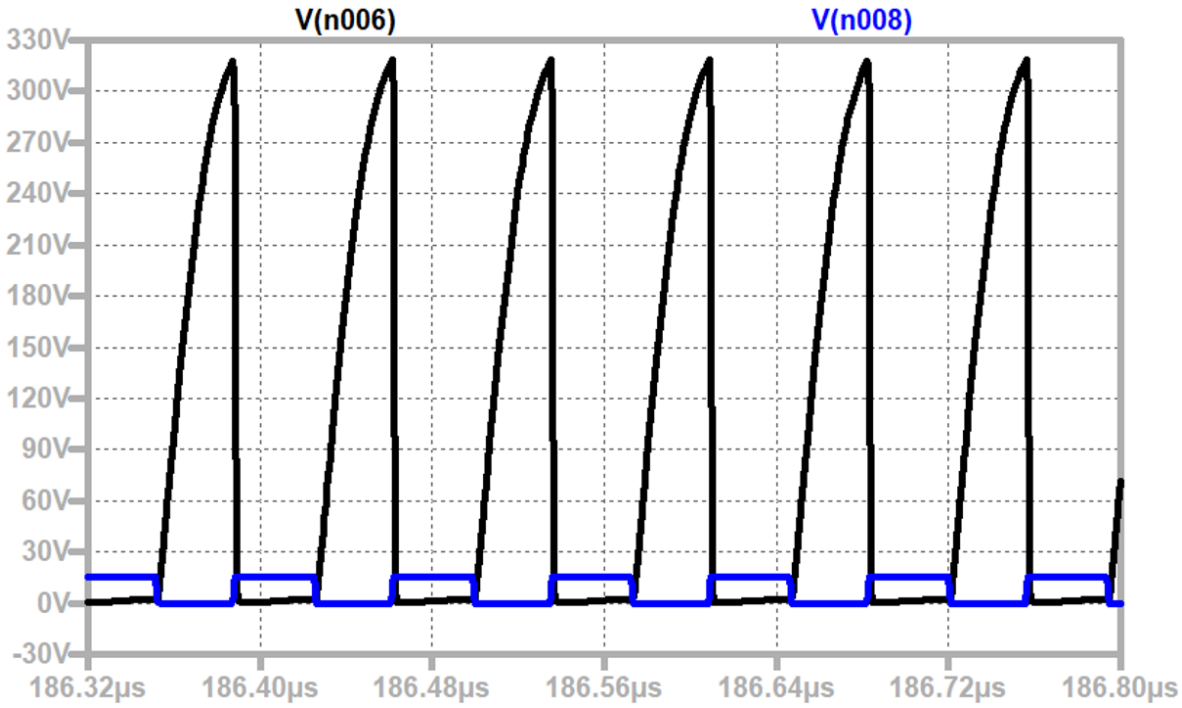

Figure 2.4: Zero Voltage Switching at 13.56 MHz

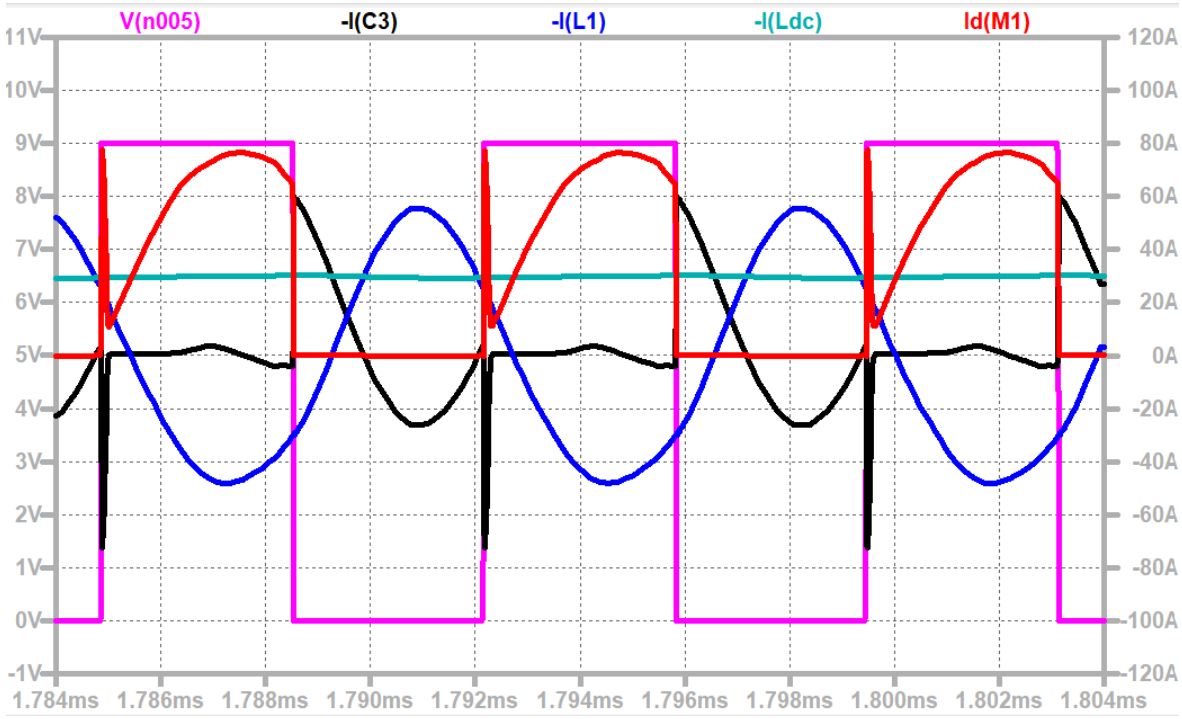

Figure 2.5: Currents in the system during switch open and close intervals

flowing into the MOSFET. Initially, when the switch is closed (MOSFET is conducting), there is a peak of current flowing out of capacitor C_3 and that same amount of current in flowing into the MOSFET. This indicates that the moment the MOSFET is turned conducting (switch is closed), the capacitor completely discharges through the MOSFET and thus has a zero voltage across it. This is also seen in the voltage graph of figure 2.4 as the voltage across the MOSFET, which is the same voltage across capacitor C_3 since they are in parallel, goes down to zero.

2.5.2 MOSFET Non-Conducting State

The instant the switch opens (MOSFET turns off), the entire behaviour of the system changes drastically. Since the MOSFET is no longer a path through which current can flow, the current behaviour changes as well. Once the MOSFET is non-conducting, there is a massive spike of current flowing into the capacitor C_3 which indicates that it is charging. This can be verified by looking the the voltage curve in figure 2.4 as it can be seen that the voltage across the capacitor C_3 increases. The current that is going into the capacitor C_3 is being supplied by L_1 as can be seen from the graph. There is still a negative current in L_1 which indicates that current is flowing out of the junction and into the capacitor. As the capacitor charges, the current going into it slowly decreases until there is no more current flowing into it when it crosses the x axis. At this point, the capacitor C_3 is fully charged and slowly starts discharging into the inductor which is shown through the proportional increase in current going into L_1 with the current coming out of C_3. The maximum amount of current going out of capacitor C_3 is at the exact same moment of the maximum amount of current going into L_1. This cycle repeats again as the amount of current going out of C_3 slowly decreases while at the same time the amount of current going into L_1 slowly decreases such that the amount of charge on the capacitor when the MOSFET is turned back on is 0. During the last quarter of cycle when the MOSFET is not conducting, the amount of current the capacitor is able to deliver decreases as the amount of charge on it is decreasing to zero. In order to have zero voltage switching, the resonant circuit must be designed in such a way that the amount of charge on the capacitor (voltage across the capacitor) when the MOSFET enters the conducting state must be zero. This is the fundamental principle of zero voltage switching. The capacitor C_3 along with the resonant circuit must work in synchronisation where current must oscillate between the inductor L_1 (and capacitor C_1) and capacitor C_3. During this half of the period, the current through the MOSFET remains zero as there is no gate source voltage being applied, thereby not allowing current to flow through the MOSFET.

2.6 Design Equation

When designing the class E amplifier, it was very important to design it in such a way that all the components work in sync in order to discharge the capacitor completely before the switch is closed again, therefore the value of the capacitors and the inductors are all the more important. When looking into equations to design the components in the circuit, Nathan O. Sokal's paper [11] provided empirical equations to help calculate the needed values for the operation of the class E amplifier.

The value of capacitor C_3 can be calculated by using equation 2.4 and C_1 and L_1 can be calculated using equations 2.5 and 2.6 respectively.

$$C_3 = \frac{1}{34.2219fR}(0.99866 + \frac{0.91424}{Q_L} - \frac{1.03175}{Q_L^2}) + \frac{0.6}{(2\pi f)^2 L_{DC1}} \tag{2.4}$$

$$C_1 = \frac{1}{2\pi fR}(\frac{1}{Q_L - 0.104823})(1.00121 + \frac{1.01468}{Q_L - 1.7879}) - \frac{0.2}{(2\pi f)^2 L_{DC1}} \tag{2.5}$$

$$L_1 = \frac{Q_L R}{2\pi f} \tag{2.6}$$

As can be seen from all of the equations above, the loaded quality factor Q_L plays a very large role in determining the values of the inductors and capacitors. The loaded quality factor is defined as:

$$Q_L = \frac{2\pi f L_2}{R} \tag{2.7}$$

The loaded Q factor signifies the resonant behaviour of the system when it is loaded with a load. The quality factor of a resonant circuit is a measuring of the energy stored in the system with respect to the average power dissipated. The bandwidth of the system is dependent on the loaded quality factor at therefore, the higher the loaded quality factor, the smaller the bandwidth of the system. The relationship between the bandwidth and the loaded quality factor is displayed in equation 2.8.

$$Bandwidth = \frac{\omega_0}{Q_L} \tag{2.8}$$

where

$$\omega_o = \frac{1}{\sqrt{L_1 C_1}} \tag{2.9}$$

The amplifiers output power depends primarily on the V_{cc} value but secondarily also depends on the value chosen for the loaded Q factor Q_L [11]. The usual value of Q lies between 1.79 and 5, which was determined analytically in Sokal's [11] paper.

Components	Values
L_{DC1}	100uH
L_1	4uH
C_3	1nF
C_1	29pF
V_{cc1}	100V

Table 2.1: The component values of the Class E Amplifier

The power output of the class E amplifier does depend on the loaded quality factor as well, as previously stated, which can be seen through equation 2.10

$$P = \frac{(V_{cc} - V_o)^2}{R} 0.576801(1.001245 - \frac{0.451759}{Q_L} - \frac{0.402444}{Q_L^2}) \tag{2.10}$$

V_0 is zero for a MOSFET, thus that term can be set to zero when calculating the output power of the system.

2.7 Conclusion

Following the design equation given in section 2.6, the values for the Class E Amplifier were found and are presented in table 2.1. These values for the system were arrived upon using the design equations presented in section 2.6.

With the amplifier values presented in table 2.1, the amplifier circuit delivers more than enough power to inductor L_1, but the design of the receiver circuit also plays a major role in the working of the entire system. Since this is a loosely coupled system, the power output at L_1 cannot be taken as conclusive evidence to state that the entire WPT system will work and deliver the needed power the load in the receiver circuit. Furthermore, attention must also be paid to the coil parameters of inductor L_1. If the coils are not designed properly, losses can occur, as will be explained in Chapter 4, in the coils themselves.

Chapter 3

Receiving Circuit Design

The fundamental working principle of the wireless power transfer circuit is that power is transferred from the primary circuit that is kept stationary on the base station, to the receiving circuit consisting of a coil and a full wave bridge rectifier which feeds the power through the battery management system to the battery (load). The inductance of the coil is determined through simulating how power is transferred between the two circuits at different coupling factors. As can be seen in figure 3.1, the receiver coil is coupled with the transmitting coil and in conjunction with the receiver capacitor, it is operating at the resonant frequency of 13.56 MHz. The signal then goes through the full wave bridge rectifier, which is created using four diodes, and is applied to the load. Since the battery requires DC power, the filter capacitor C_4 is used to smoothen out the AC signal and supply a clean DC signal to the load (battery).

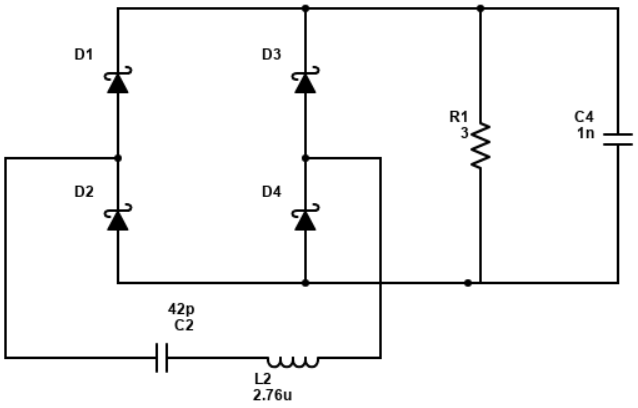

Figure 3.1: Receiver Circuit with Diode Circuit

3.1 Series Resonant Circuit

In figure 3.1, the resonant inductor L_2 and C_2 form the series resonator that will be coupled to the primary system and use inductive resonant coupling to transfer the power to the battery (Resistor R_1). L_2 will be the receiving coil that will be resonantly coupled to inductor L_1 in the class E amplifier circuit. The value of L_2 was found through using simulation based analysis to be able to generate enough AC voltage such the RMS of the signal would be sufficient to charge the battery (14.4 V). If the self inductance of the inductor was too large, the overall coil parameters would be too large to fit on the drone without compromising the payload capacity significantly. If the coil inductance was too small, it would not be able to generate enough AC voltage to meet the power requirements of the battery. Therefore, looking into previous papers, most of them had receiving coils around 50 - 60 % the size of the transmitting coil, therefore, that was used as a baseline to experiment with values to find the optimal size.

3.2 Diodes

The actual diodes being used in the circuit are of extreme importance as their threshold value should be as low as possible to avoid major switching losses. In order to achieve this, Silicon Carbide Schottky Diodes are used as they have a substantially lower forward drop voltage than conventional silicon PN junction diodes. In PN junction diodes, the knee voltage (forward drop voltage) is usually between 0.6 and 0.9, depending on the doping concentrations. In a standard PN junction diode, semiconducting materials are used in both the P and the N type layer, where the P type layer is doped with excess electrons and the N type layer is doped with extra holes [12]. Thus the knee voltage is determined by how much energy is required for a hole to go from the N type region through to the dielectric material and again through into the P type region. Therefore, there is a certain amount of voltage required before diode goes into conduction. The main difference between the Shottky diode and a PN junction diode is that one of the semiconducting layers is replaced with a metal electrode, which is then bonded to an N type semiconductor. Due to this there is no depletion layer between the metal and the semiconductor thereby classifying these types of diodes as uni-polar diodes. In this specific application, a Silicon Carbide diode is used which has a knee voltage of only around 0.3 volts. The forward voltage of the diode is of extreme importance in this case as power will be dissipated on the diode every half cycle, and since the frequency of the signal is 13.56 MHz, that will be once every 73.74 nanoseconds. Since there are four diodes in the full bridge rectifier, that will equate to around 1.2 V drop over all of the diodes combined every

Components	Values
L_2	2.8uH
C_2	42pF
R_1	3 Ω
C_4	1nF

Table 3.1: Component Values of the Receiving Circuit

cycle.

3.3 Load

The battery is represented by resistor R_1. For the DJI F550, the required voltage on the battery is around 14.4 Volts with a total power of around 75 Watts which leads to a battery internal resistance of around 3 ohms.

3.4 Filter Capacitor

The capacitor C_4 placed in parallel with the load is there to balance out the fast changing positive AC signal into a much smoother DC signal that can be used to charge the battery. This is done by making sure that the value of the capacitor is big enough such that it does not discharge during the transition from one half cycle to the next. The voltage over the charged capacitor is then the voltage over the load which is a DC signal. If the capacitance of the parallel capacitor is too large, then it takes much longer for the capacitor to charge completely and thereby the voltage over the load will gradually increase, but there will be little to no ripple in the steady state of voltage. If the capacitance is too small, then the capacitor charges quite quickly but also discharges between the half cycles, thereby having a small ripple in the steady state. This is demonstrated in figure 3.2, where the value of the capacitor was 0.1 micro farad and the size of the capacitor in figure 3.3 was 0.1 mili farad. As seen, in figure 3.2, the capacitor reaches it fully charged state much quicker than the capacitor in figure 3.3, but since the size of the capacitor is too small, it oscillates even in the steady state, which is not desired.

3.5 Conclusion

The values of the components in the receiving circuit are presented in table 3.1.

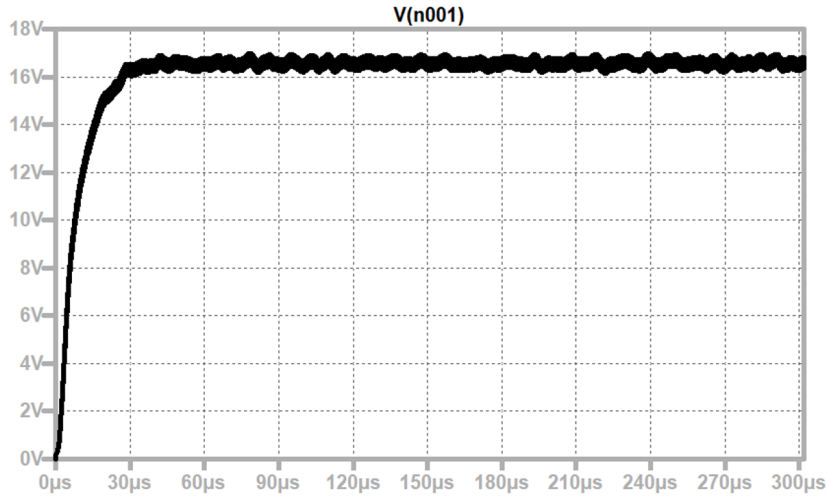

Figure 3.2: Size of the capacitor is too small

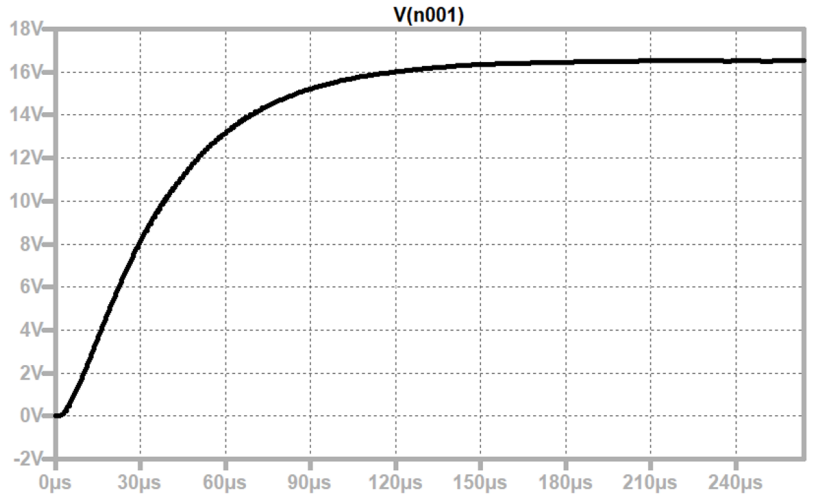

Figure 3.3: Size of the capacitor is appropriate

With these values and the use of Silicon Carbide diodes, the 90 Watts of power was delivered to the load and the battery was charged in an hour. The components of major importance are the series resonant circuit as well as the diodes used in this implementation. Minimising the losses on the diodes throughout each cycle was critical to the overall efficiency of the system, thus the choice of Silicon Carbide diodes was made due to their low knee voltage. The resonant circuit values (inductor and capacitor) must also be chosen such that they resonate at 13.56 MHz and the size of the inductor must be chosen such that the inductor is capable of outputting the necessary power. Ideally, the system would have had much more power as the class E amplifier was able to output significantly more than that received by the load. However, due to the low coupling factor (loosely coupled system) only a fraction of the power being transmitting by the amplifier is received by the load.

Chapter 4

Charging Pad Design

The design of the coils that are used in the transmitting and receiving circuit are very important in the power transmission capabilities of the system and play a large role in the efficiency of the system as well. By using proven design equations and intelligent design parameters, the performance of the coils can be optimised to provide the highest possible power output capabilities. Coils with the same inductance values can be formed in many ways, but some are better design decisions than others, thus this chapter will focus on what aspects of the coils design were taken into account and how they affect the overall performance of the WPT system.

4.1 Structure

The chapter will begin by discussing the important factors when looking at determining coil parameters which will be followed by potential designs that could be used. Lastly, the different design equation used to create the coils are discussed along with reasoning behind why certain parameters were chosen for use in this specific WPT system. Since all WPT systems are different, one set of coil parameters cannot be used in another system as the resonant frequency, power transfer capabilities and many more things affect the design process. Therefore, proper reasoning is given to justify the use of specific values and parameters.

4.2 kQ Factor

When designing the coil parameters for a resonant inductive wireless power transfer (WPT) system, the kQ factor is of the utmost importance as it dictates the effectiveness of the power transfer [4]. Effectiveness can be broken down into power output and efficiency, both being affected by the kQ factor. The kQ factor consists of two separate parameters, known as the coupling factor (coupling coefficient) k, and the

quality factor Q. When two coils are placed in close proximity of each other and an AC current is supplied to the transmitting coil, some of the magnetic flux generated by that coil will penetrate the receiver coil thereby induce a electromotive force. The coupling factor can be used as a mean to quantify how much of the flux generated by the transmitting coil penetrates the receiving coils and contributes to power transmission [3]. A coupling factor of 1 indicates that the two systems are well coupled and that all of the flux generated by the primary coil penetrates the secondary coil and generates an electromotive force. On the other hand, a coupling factor of 0 indicates that the two coils are independent of each other and that the behaviour of one does not influence the behaviour of the other. Equation 4.1 illustrates this relationship where L_{11} and L_{22} are the self inductances of the transmitting and receiving coil respectively and L_{12} is the mutual inductance of the two coils.

$$k = \frac{L_{12}}{\sqrt{L_{11} \cdot L_{22}}} \tag{4.1}$$

k is the coupling factor and can be described using the self inductances of the two coils along with the mutual inductance. Mutual inductance is the ”interaction of one coils magnetic field with the on another as it induces a voltage in the adjacent coil [13].” By observing the terms of equation 4.1 [4] , it can be noted that the coupling factor of the system and the mutual inductance are proportional to each other, therefore an increase in the coupling factor will result in an increase in the mutual inductance of the system.

Similarly the quality factor (Q factor) is also a very important criterion when looking at the performance of a WPT system. The Q factor is a way of measuring the performance of a resonant circuit [14]. The Q factor is a dimensionless number that is used to describe the damping in a circuit and is a good measure of how good the oscillator oscillates at its resonant frequency as shown in figure 4.1. It can be mathematically defined as:

$$Q = \omega \frac{\text{Energy Stored}}{\text{Average power dissipated}} \tag{4.2}$$

The Q factor of each of the coils is expressed through equations [4] 4.4 and 4.5 while the combined Q factor of the entire system is given through equation 4.3.

$$Q = \sqrt{Q_{primary} \cdot Q_{secondary}} \tag{4.3}$$

$$Q_{primary} = \frac{\omega \cdot L_{primary}}{R_{primary}} \tag{4.4}$$

$$Q_{secondary} = \frac{\omega \cdot L_{secondary}}{R_{secondary}} \tag{4.5}$$

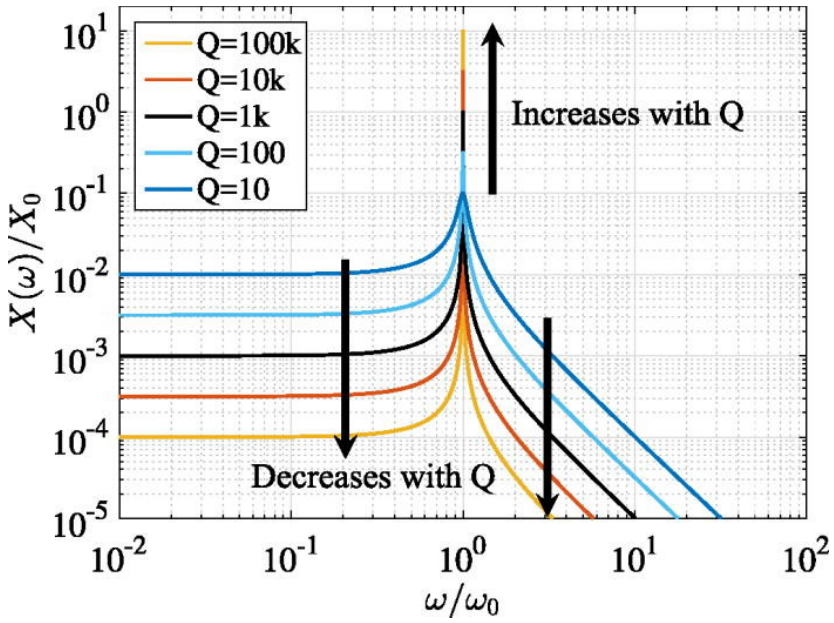

Figure 4.1: Different possible Q factors for a given system. [2]

In both equation 4.4 and 4.5, the self resistance of the coils plays a role in the overall quality factor of the circuit. This R value can only be changed by changing the material of the coil themselves as better conductors, such as gold, have a lower internal resistance as compared to other metals like copper. The resistance of the material plays a significant role in the Q factor of that system because the power that will be dissipated is linked to the amount of resistance in the component. The more innate resistance the material has, the more power will be lost in the material, thereby decreasing the resonant response of the system. The self inductance L for a circular planar coil is described through equation 4.10.

4.3 Misalignment, Coupling Factor and Coil Shapes

The coupling factor between the two coils and the alignment of them are very much interrelated and this relationship can be seen through figure 4.2 [3]. As figure 4.2 demonstrates, the coupling factor of the two coils increases as the coils are axially aligned and brought very close to each other (top left of figure 4.2) and decreases as the coils are moved away from each other and as the axial misalignment between the two is increased (bottom right of figure 4.2). The coupling factor is of major importance to the WPT system as discussed in section 4.2 and therefore, the alignment of the two coils places a large part in that.

As the coils come closer together, the flux that goes through the second coil is higher, as there is less of an air gap between the two coils where the flux lines

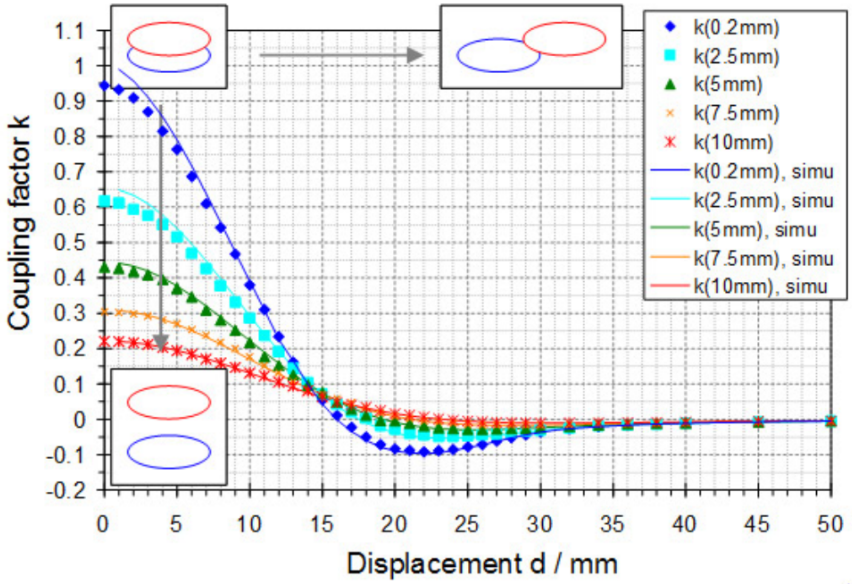

Figure 4.2: Relationship between Coupling Factor and axial misalignment of both the coils. Top left indicates coils are small air-gap and no axial misalignment (high coupling factor), whereas, bottom right indicates large axial misalignment and large air-gap between both coils (low coupling factor). [3]

can have different reluctance paths leading to lowered efficiency. Since magnetic flux lines always form a form a closed loop, the path of the lines depends on the reluctance of the materials surrounding it. Air and vacuum are known to have a very high reluctance, whereas ferrite has a very low reluctance, thereby making it very good in guiding flux lines all in the same direction. However, since the WPT system being discussed in this paper is going to consist of air core coils, the reluctance path of the flux lines plays a large role in the overall efficiency and power transfer of the system. The flux lines generated from the edges of the coils will have a small circular path as they will choose the path of least reluctance, where as the flux lines generated from the AC current near the centre of the coil will generate much longer paths thereby also going through the secondary coil and generating an electromotive force in the secondary coil. As the coils are moved further apart, more and more of the flux lines will have paths which do not go through the secondary coil, thereby decreasing the mutual inductance leading to a lower coupling factor. This is one of the major principles behind why the coupling factor of the system decreases as the distance and the misalignment between the two coils increases. This is also one of the driving principles behind trying to get the primary and the secondary coils as coil to each other as possible.

Furthermore, the geometry of the coil used for inductive wireless charging will

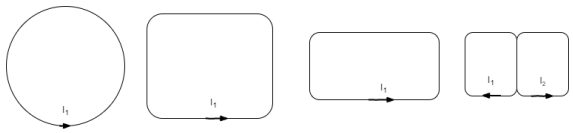

Figure 4.3: Different Coil Geometries a) Circular Coil b) Square Coil c) Rectangular Coil d)Segmented Square Coil

also have a large effect on the efficiency and the power transfer capabilities of the system. There are multiple different coil geometry as shown in figure 4.3 that could be employed in a wireless power transfer system for drones ranging from circular coils to rectangular coils all the way to conical coils. Each of these different geometries bring their own benefits and drawbacks. Conical coils, for example, have a higher directivity of their flux lines [15], thereby making them beneficial in application that require high directivity of the transmitting coil. This is very beneficial if the coils of the receiving and the transmitting antenna are always going to be perfectly aligned as it will result in a high flux linkage, but quickly becomes an inefficient coil topology if the transmitting and receiving coils are even slightly misaligned. Conical coils are not robust for different amounts of alignment, making them a less favourable choice in WPT applications where alignment between the two coils cannot always be guaranteed. Similarly both the square and the rectangular coils display fringing effects, where the flux lines go outwards from the desired path, due to the sharp turns present in the coils, which decreases the overall efficiency of the system. Due to the distortion of the magnetic field in the case of square and rectangular coils around the corners, the magnetic coupling is inferior to that of a circular coil as demonstrated in figure 4.4 [4]. All in all, as the coil area increases, the magnetic coupling between two circular coils was found to be the best [4], as shown in figure 4.4 thus it would be the ideal candidate for implementation in a charging a drone wirelessly.

4.4 Ferrite Pads

The addition of a ferrite pads below the transmitting coil also vastly enhances the coupling between the two coils as it prevent leakage of the magnetic field and improve the self inductance and mutual inductance of the coils [4]. As discussed in section 4.3, the reluctance of air is very high, but the reluctance of ferrite is relatively low, ensuring that most of the flux lines go through the ferrite pad and are then redirected upwards towards the receiving coil. Furthermore, ferrite has a high permeability, allowing the flux lines to easily pass through the material without generating high losses. Many different materials could be used as pads but ferrite brings the most benefits due to its high relative permeability and low losses at high fre-

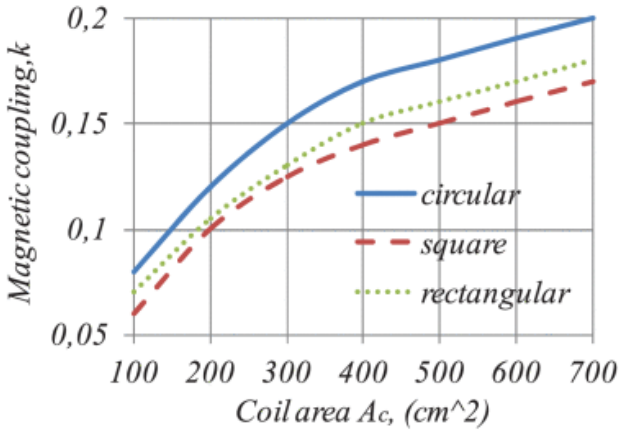

Figure 4.4: Coil Area vs Magnetic Coupling factor for circular, square and rectangular coils [4]

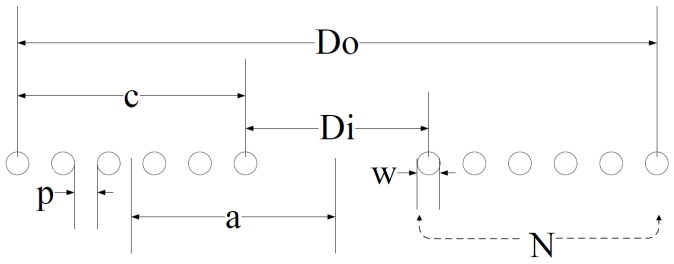

Figure 4.5: Cross section of a flat spiral coil [5]

quencies [4]. However, the idea of using ferrite pads was not investigated further due to lack of resources to simulate the behaviour of the system with ferrite pads, as well as the increasing cost and complexity of the entire system. Therefore, this was left as a future work that could the implemented in the system to improve overall performance.

4.5 Design Equations

When starting to design coils, it is first important to look at how much current the coils are expected to handle and what material of wire needs to be used to satisfy that condition. Since the system needs to deliver at least 8.6 Amps of current, Litz AWG 12 wires [16] were chosen as they would minimise the skin effect. The cross section of a circular coil is given in figure 4.5 and shows the different parameters of the coil that are of relevance to its performance.

That outer radius shown in figure 4.5 is Do along with the inner radius being defined as Di. The width of the coil w is determined by the width of the Litz AWG

12 wire which is 2.053mm. The pitch, p, as illustrated in figure 4.5, also plays an important role in the quality factor of the system. If pitch is too small, the proximity effect losses will dramatically decrease the quality factor of the system which will hinder the efficiency and the power output of the system. When placing AC current carrying wires in close proximity to each other, the proximity effect losses must be taken into account. These losses are caused by the alternating flux in a conducting material caused by the alternating flux in the nearby conducting material. This flux is not desired can produce circulating eddy currents which will result in the apparent increase in the resistance of the wire [17]. From there equation 4.6 is derived where the outer radius and the pitch angle along with the width of the wire can determine the inner radius of the coil [5].

$$D_i = D_o - 2N(w + p) \tag{4.6}$$

The length of the wire needed to construct this certain coil [5] was determined by using equation 4.7. It is important to know the actual length of the coil as it is needed to buy the right amount of Litz wire to build it as well as to calculate the DC resistance as shown in equation 4.12.

$$l = \frac{1}{2}N\pi(D_o + D_i) \tag{4.7}$$

Equation 4.8 and 4.9 [5] are of importance because the inductance equation given in 4.10 is found to be accurate for most geometries except when the geometry has very few turns, when the pitch angle is relatively large compared to the wire diameter ($p >> w$) and when $\frac{c}{a} < 0.2$ [5]. Therefore, it was ensured that the coils did not have very few turns and that the pitch angle is not extremely large with respect to the wire diameter. It was also ensured that the $\frac{c}{a}$ ratio was not smaller than 0.2 as these equations do not hold for values of $\frac{c}{a}$ less than 0.2.

$$a = \frac{1}{4}(D_o + D_i) \tag{4.8}$$

$$c = \frac{1}{2}(D_o - D_i) \tag{4.9}$$

Having determined all of the physical parameters of the coil, the inductance [5] of the coil was determined using equation 4.10.

$$L[H/m] = \frac{N^2(D_o - N(w + p))^2}{16D_o + 28N(w + p)} \cdot \frac{39.37}{10^6} \tag{4.10}$$

Thereafter, the resonant capacitance [5] can be determined to be using equation 4.11. This capacitor plays an important role in the system as it, along with the inductor, allows for resonant wireless power transfer. The resonant frequency of the

transmitter system and the receiver system are tuned in such as way that they are both operating at the same resonant peak.

$$C = \frac{1}{2\pi f^2 L} \tag{4.11}$$

$$R_{DC} = \frac{l}{\sigma\pi(w/2)^2} \tag{4.12}$$

$$\delta = \frac{1}{\sqrt{\pi f \sigma \mu_o}} \tag{4.13}$$

The DC resistance and the skin depth [5] can both be approximated using equations 4.12 and 4.13 respectively. The DC resistance is the innate resistance of the material to and increases as the length of the wire increases as shown in equation 4.12. The width of the wire is fixed, as well as the conductivity of the wire, thus the only factor affecting the DC resistance of the wire is its length. The AC resistance which is expressed through the skin depth resistance is affected by the frequency of the system. The higher the frequency of the system the more prevalent the skin depth resistance becomes. The skin depth effect occurs in AC signals where the current density does not flow uniformly through the wire rather builds up around the outside of the wire and decreases exponentially as the distance from the surface increases. To prevent this effect from causing unnecessary resistance, Litz wire is used as it consists of multiple strands of wire within one larger wire, thereby decreasing the width of each strand decreasing the skin depth resistance. Since all the wires have a smaller diameter, the AC signal can penetrate through more of the material.

The total resistance, which is a combination of the DC resistance and the skin depth resistance, is calculated using 4.14. In order to have a high Q factor, this total resistance should be reduced as much as possible.

$$R_{tot} = R_{DC}\frac{w}{4\delta} = \sqrt{\frac{f\pi\sigma}{\mu_o}}\frac{wN(D_o - N(w+p))}{w} \tag{4.14}$$

4.6 Conclusion

After understanding how the operation of the class E amplifier and the coils are critical to the operation of this WPT system, the parameters of both the transmitting and the receiving coils is presented in table 4.1.

The inductances of the coils are both determined by the requirement of the inductors in the transmitting and the receiving circuits respectively, but the actual dimensions of the coils are determined through the design equations presented in section

	Transmitting Coil	Receiving Coil
Inductance:	4.0uH	2.8uH
Number of Turns	4.0	4.0
Pitch (meters)	0.0187	0.0057
Wire Diameter (meters)	0.0021	0.0021
Inner Diameter (meters)	0.1340	0.0876
Outer Diameter (meters)	0.3000	0.1500

Table 4.1: Properties of Transmitting and Receiving Coil

4.5. In order to maximise the quality factor in these coils, some simulated studies were conducted to see how the quality factor could be maximised while achieving the necessary inductance values.

Chapter 5

Models

5.1 T- Model

In order to more accurately calculate values for the receiving and transmitting coils, the IWPT circuit was simplified into an equivalent circuit as shown in figure 5.1, which was very similar to the equivalent circuit of a transformer. Inductor L_3 aims to model the mutual inductance between L_1 (transmitting coil) and L_2 (receiving coil), as it is calculated by using the mutual inductance formula 5.1.

$$M = k\sqrt{L_1 L_2} \tag{5.1}$$

k is the coupling factor which dictates how well the two circuits are ”connected” to each other and L_1 and L_2 are the self inductances. Since this IPT is a loosely coupled system, the coupling factor k is usually in the range of 0.1 to 0.3. The values of C_1 and C_2 are chosen using the resonant equations of a series-series compensation topology discussed in section 2.5

When initially designing the class E amplifier circuit, the T model was used as it is a good representation of how the actual circuit will behave with certain component

Components	Values
R_1	1mΩ
C_1	20pF
L_1	4uH
R_2	1mΩ
C_2	42pF
L_2	2.76uH
R_3	3Ω
L_3	0.66uH

Table 5.1: Simulated values in the T- Model

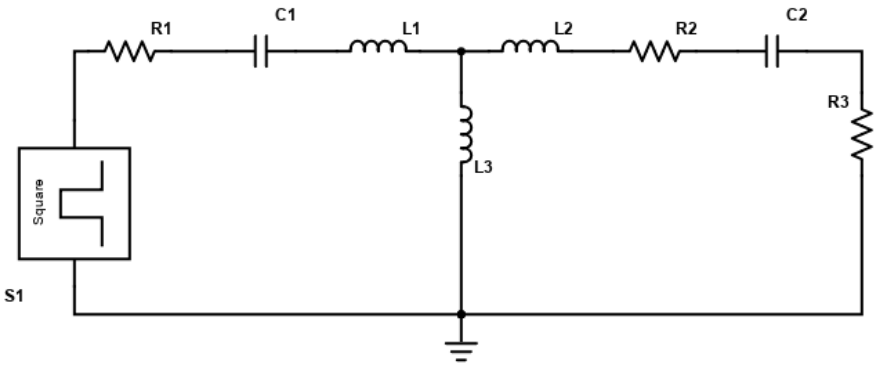

Figure 5.1: Equivalent circuit of magnetically coupled coils. L_1 is the transmitting coil, L_2 is the receiving coil and L_3 is the mutual inductance between the two coils. R_1 and R_2 are the parasitic resistances of the circuit while R_3 is the load (battery).

values. Since the coupling did not have to be simulated between two coils, using this method was much more time efficient and yielded result that provided a good indication of how the actual system would perform. The values used in the model are shown in table 5.1 and the voltage and current at the load are displayed in figure 5.2. The RMS voltage is around 18 Volts and the current is around 7 Amps, which equates to around 126 Watts RMS. The results of the T-Model simulation will not be exactly the same as those seen in the actual circuit model, but it will give a good idea of how the circuit will behave. Since there is no rectifying bridge, no MOSFET and other components, the actual power output from the circuit will be less than that shown in the T- model simulations.

5.2 Series- Series Inductive Power Transfer Circuit

A series- series resonant topology, shown in figure 5.3, was also created to see the frequency behaviour of the system for differing coupling factors to simulate real world use.

Inductors L_1 and L_2 are coupled together and the input for the circuit is chosen to be a 100 V sine wave. As the frequency was swept from 5 MHz to 30MHz, the circuit was tested for a range of coupling factors to see how it would react and to understand the circuits behaviour for different frequencies. The circuit's performance can be measured in a few substantial ways that can unveil the efficiency and the power transfer of the system. One of these methods is known as the S-Parameter which describes the relationship between two ports in an electrical system. In an electrical

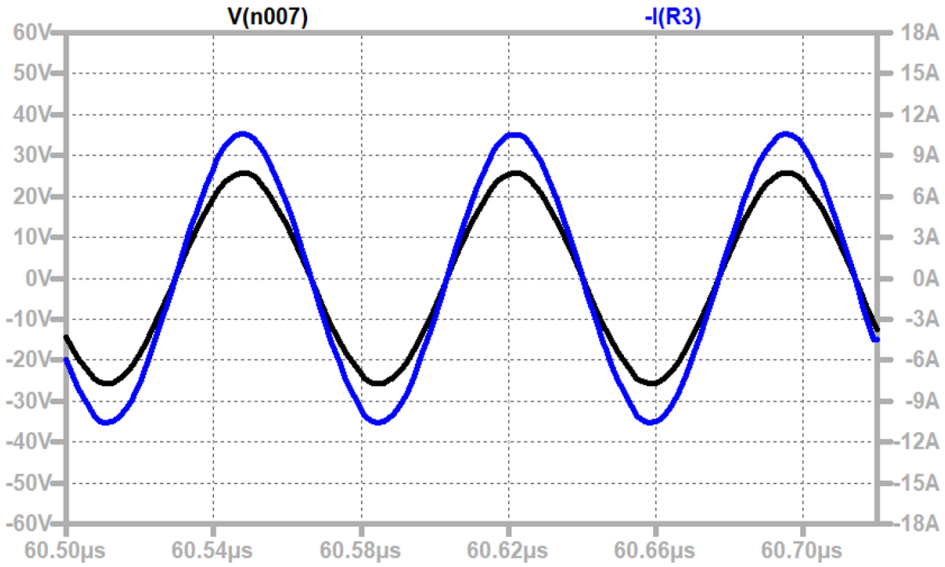

Figure 5.2: RMS Current and Voltage in the T- Model system. RMS voltage is 18 V and RMS current is 7 Amps.

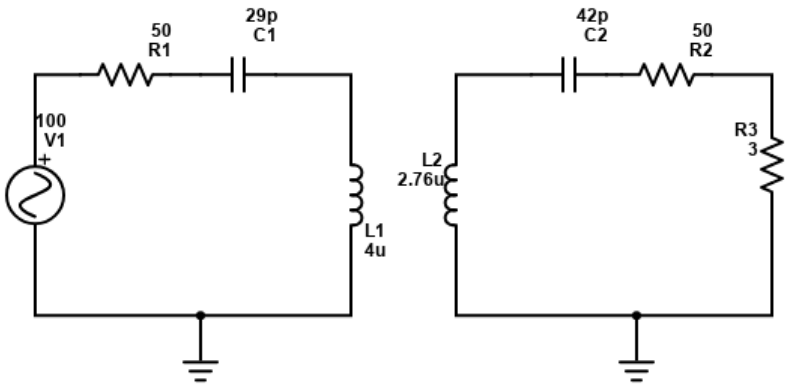

Figure 5.3: Series- Series Resonant Circuit. L_1 and L_2 are the coupled coils and C_1 and C_2 from the series circuits for the transmitting and the receiving side respectively.

system, a port is defined as place where voltage and current can be delivered. Thus in the case of the WPT system, it can be defined as a 2 port system with one port being the output from the transmitting antenna and another port being the receiving antenna [18]. The S-parameter that is of importance in this circuit is the S_{21} parameter which represents the power delivered from Port 1 to Port 2 (Power from transmitting coil to receiving coil). The S_{21} parameter can be expressed in the following way for a WPT system.

$$S21 = 2\frac{V_{Load}}{V_{Source}}\sqrt{\frac{R_{Source}}{R_{Load}}} \tag{5.2}$$

Equation 5.2 gives the power that is delivered to the load when compared to the source voltage.

The circuit also showed interesting frequency behaviour when the coupling factor was changed from 0.1 to 0.6. Since this is a loosely coupled system, the coil parameters and the circuit design have been made with a coupling factor of 0.4 as that was the maximum achievable coupling factor found in other papers for loosely coupled WPT systems. These results will be discussed in the following Chapter, aptly named Sensitivity Analysis.

Chapter 6

Sensitivity Analysis

Sensitivity Analysis is an important tool that simulates how the system will behave when different parameters of the system change due to known or unknown circumstances. The 3 parameters of importance that could vary throughout the course of the WPT system are the coupling factor, the resonant capacitor value, and the load on the system.

6.1 System Load

Figure 6.1 displays how the impedance curves of the system changes as the coupling factor of the system is varied. The dotted line plots can be ignored as they are plotting the phase of the signal and that is not of relevance for this application. The black plot is the system impedance of a coupling factor of 0.1, and the blue plot is for the system designed coupling factor of 0.2 and so on. Since the circuit uses a Series- Series topology, as explained in section 2.5, the impedance at the resonant peak will be a minimum which is what is seen in figure 6.1.

The system load analysis is a useful way of seeing how the resonant frequency of the system would change as function of the coupling factor. This idea is seen in figure 6.2 where the coupling factors are the x- axis and the y- axis is the systems frequency deviation from 13.56 MHz.

Since the system is designed for a coupling factor of 0.2, the frequency deviation is 0, but as the coupling factor increases, the deviation from the desired frequency of 13.56 MHz increases and it resonant peak shifts. Knowing this information is crucial in designing a proper control system that accurately adjusts the necessary parameters to tune the system back into resonance. This can be done by either changing the frequency of the MOSFET driver and thereby adjusting the DC choke inductor or by tuning the resonant capacitor.

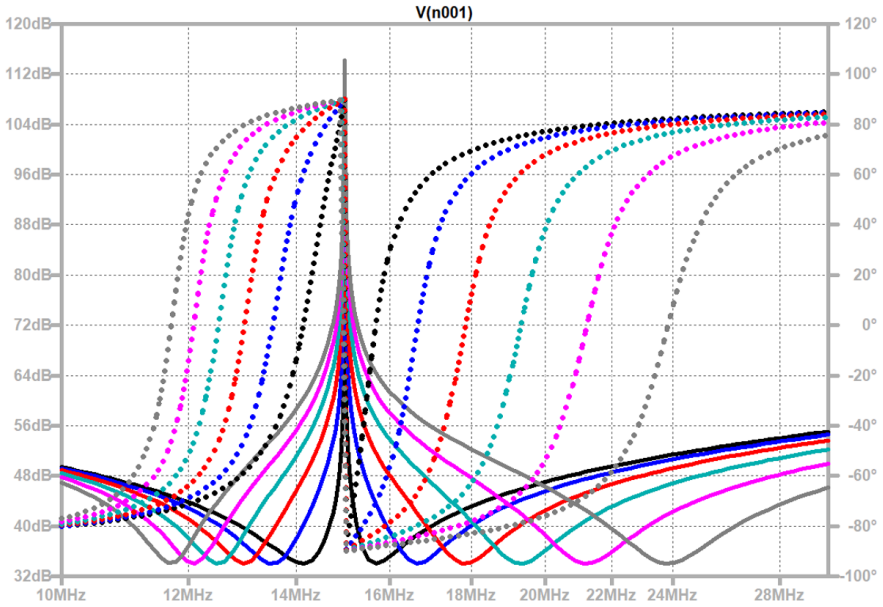

Figure 6.1: How the change in the coupling factor affects the frequency of minimum impedance of the system. Blue curve is k = 0.2 and impedance of the system is lowest at 13.56 MHz (Ideal). Red plot if k = 0.3 and so on.

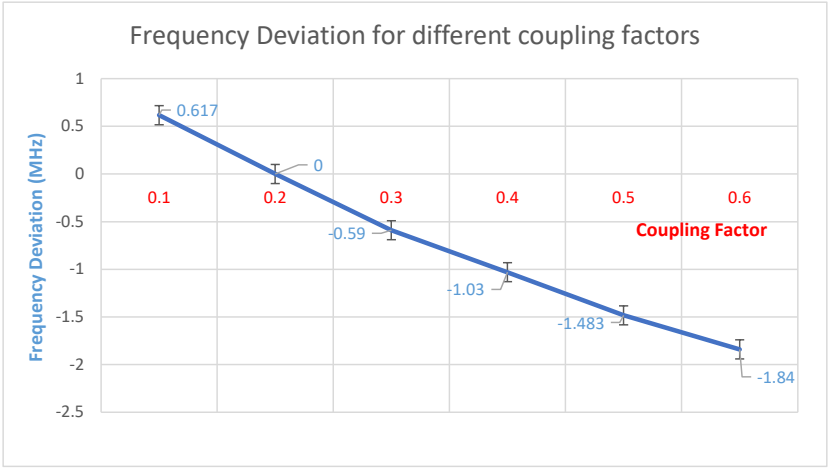

Figure 6.2: The relationship between the coupling factor of the system and the frequency deviation experienced by the system from 13.56 MHz. X- Axis (Red) are the different coupling factors and y- axis are the frequency deviations.

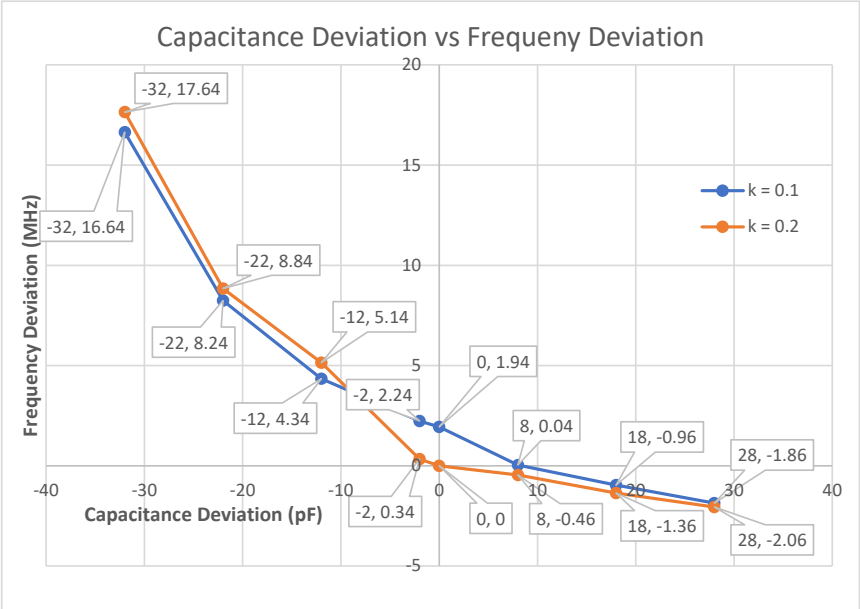

Figure 6.3: Capacitance Deviation vs Frequency Deviation for k=0.1 and k = 0.2

6.2 Resonant Capacitor Analysis

Doing a sensitivity analysis on the resonant capacitors is of high importance because it provides the designer with the understanding of how the ageing of the components could lead to the different behaviours in the circuit. The value of the capacitance will vary due to the ageing of the circuit, the temperature cycles that it goes through and other more complicated reasons, thus understanding how the system will behave to capacitance variations is useful to know. [19]

More importantly, there are only a few capacitors that are currently available on the market that are made for high energy resonant applications. The values required for a resonant capacitor in WPT applications are usually quite small, therefore it is difficult to find the exact required capacitor value [19].

As shown in figure 6.3, the frequency deviation of the circuit was plotted against the deviation of the resonant capacitor to see how the much the frequency would deviate from desired one as the value of the capacitor fluctuates. As displayed by both figures, the curve resembles a $\frac{1}{\sqrt{X}}$ relationship which makes sense as the frequency and the capacitance are related with a $\frac{1}{\sqrt{C}}$ relationship. This illustrates that for a coupling factor of 0.1, the frequency deviation is less than the frequency deviation for the system with a coupling factor of 0.2. For every capacitance deviation, the appropriate frequency deviation is lower, which suggests that the system is more

robust to capacitance deviations for lower coupling factors.

6.3 Coupling Coefficient

The coupling coefficient is one likely the parameter that will affect the performance of the circuit the most as it dictates how well the two coils are aligned and how much flux from generated from the AC signal in the primary coil is generating an AC signal in the secondary signal. The behaviour of the circuit for different coupling coefficients can be seen from figure 6.4. The blue curve is the resonant frequency of the circuit for a coupling factor of 0.2. As the coupling factor of the system changes, the reflected impedance of the secondary circuit on the primary circuit also changes, thereby shifting the resonant frequency of the system. As seen, when the coupling factor is increased or decreased, the circuit demonstrates a frequency behaviour where the resonant peak shifts as the coupling factor changes. This principle is demonstrated through figure 6.4.

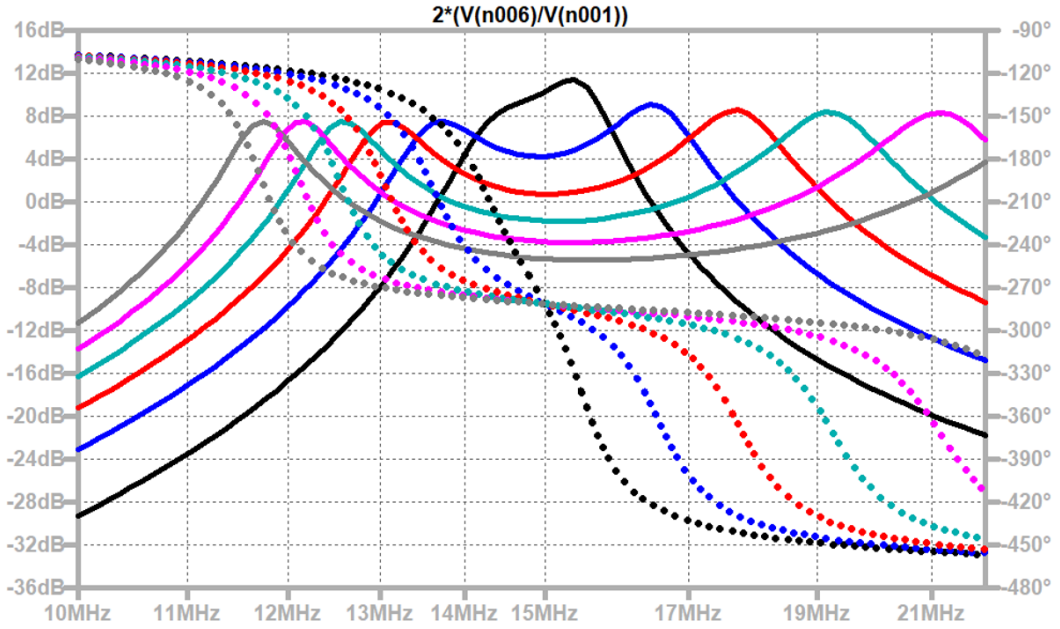

Figure 6.4: S21 parameter for coupling factors of the system. Blue plot is the system for a coupling factor of 0.2. Red plot is for a coupling factor of 0.3 and so on.

In figure 6.4, there are multiple curves that represent coupling factors from 0.1 till 0.6. The black curve represents the power received by the load when the coupling factor is 0.1, and the blue curve is the output power at a coupling factor of 0.2 and so on. The dotted lines in figure 6.4 can be ignored for this application since they are describing the phase of the signal for each of the system for the different coupling

factors. The location of the resonant peaks on the frequency spectrum changes based on the coupling factor between the transmitting and the receiving network. This has a major influence of the power transmission capabilities of the system as a change in the coupling factor would move the resonant peak to a different frequency causing the system, at 13.56 MHz, to no longer be operating at the resonant frequency, leading to lower power transmission. Since the impedance of the system is the lowest at the resonant frequency, the best results will be achieved when the system is operating at resonance. The system values were initially designed for a coupling factor of 0.2 since that is the most common coupling factor for loosely coupled systems. Any coupling factor higher or lower will lead to an inefficiency system unless compensated for by an external control system. It would require a control system that could adjust the needed values in the system to ensure that it always operates at the point of lowest impedance and the point of maximum power output.

Chapter 7

Results

Due to the ongoing situation with the COVID- 19 pandemic, access to testing facilities were very limited, therefore only simulation testing was possible. Following the procedure outlined in Chapters 2 and 4, values for the entire system were found and verified using LT Spice. The values of the components in the class E amplifier model are displayed in table 2.1.

The values of all the components were chosen using the design equations presented in Chapter 2 and thereafter were tested through simulation using LT Spice to see the appropriate power could be delivered to the load. The value of the capacitor C_2 is directly dependent on the value of inductor L_2, and the value of capacitor C_3 in figure 7.1 was approximated using the design equations but then was later tweaked through simulation. It was preferred to keep the DC supply voltage as low as possible to achieve the required power output, and that could be done by refining the coil parameters and ensuring that the circuit is always operating at a resonant peak, regardless of the coupling between the two circuits.

On the other hand, creating the secondary circuit was a much simpler process, but not without its challenges either. Conscious decisions were taken in order to ensure the efficient working of the secondary circuit. The diode bridge used Shottky didoes as explained in section 3.2, in order to decrease the switching losses and switching time. As explained in section 3.4, the value of the capacitor C_4 was also tweaked through iteration and simulation. This process was shown through figure 3.2 and figure 3.3.

The entire circuit diagram can be seen in figure 7.1, where both the transmitting circuit and the receiving circuit are shown. Inductors L_1 and L_2 are both magnetically coupled to each other and capacitors C_1 and C_2, respectively, are resonant capacitors used to resonant the circuit at 13.56 MHz.

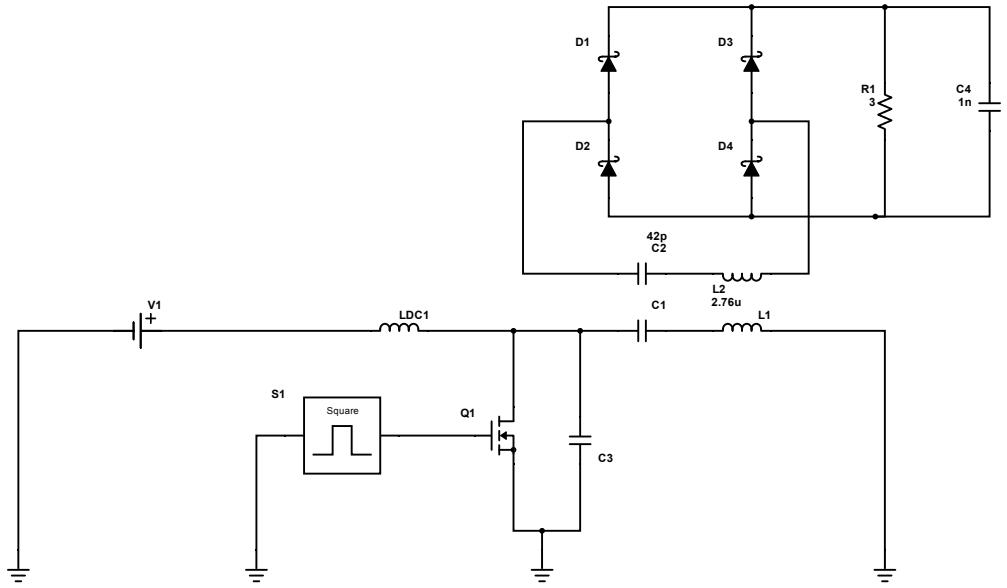

Figure 7.1: Complete WPT system diagram

7.1 Coil Parameters

After finalising the circuit values for the class E amplifier and the secondary circuit, the inductance values where then used to craft the coil properties required to generate the needed inductance. This was done using the equations presented in Chapter 4 and ultimately resulted in the following coil properties for both the primary and the secondary coil shown in table 4.1. A MATLAB script was written, which calculated the optimum values of all the parameters for a given inductance value, outer diameter, and wire diameter.

7.2 Power Output

The main goal of this entire system was to charge a DJI drone with at least 75 Watts of power such that it would be completely charged within one hour. With a 100 V DC power supply the system, at a coupling factor of 0.2, which is quite an appropriate coupling factor for a loosely coupled system, the system was able to deliver around 90 Watts of power to the battery at a voltage of 16V. The DC supply voltage can even be decreased to a lower value and still sufficiently meet the requirement set for this WPT system, but this will yield poorer results if the coupling factor drops below 0.2.

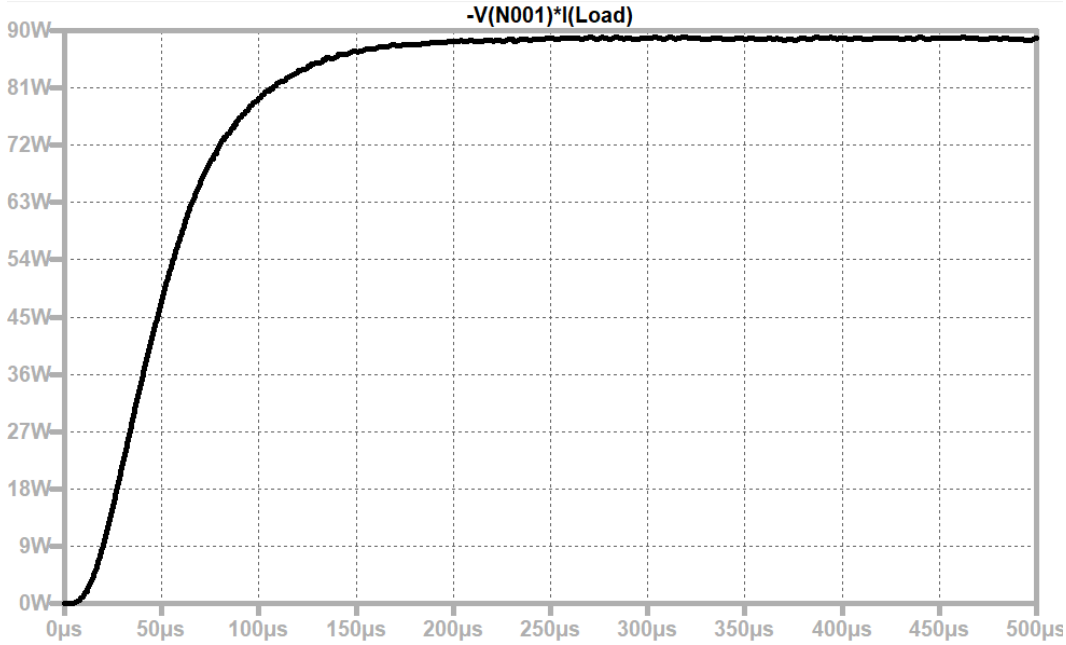

Figure 7.2: The total power output of the circuit

7.2.1 Efficiency

When simulations were done to see the overall efficiency of the system, the results were mixed. The system had an efficiency of around 10% at a coupling factor of 0.2, which increased to around 50% for a coupling factor of 0.4. However, when seeing where the losses were occurring, it was noticed that at every switching point on the MOSFET, there was a massive power spike for around 1ns. After the original MOSFET was replaced by a Gallium Nitrate one, the efficiency of the system 60%. It was concluded after a discussion with Dr. Venugopal, that this might be a simulation error and not much attention should be paid to this number. Due to the unavailability of the labs, testing was not able to be done on the system to see what the actual efficiency of the system will be.

7.3 Power Output Relationship to Coupling Factor

As illustrated in figure 6.4, as the coupling factor of the system changes, so does the S_{21} parameter, which indicates that the power output from port 1 to port 2 also changes. As the coupling factor increases or decreases, the resonant frequency shifts from 13.56 MHz to other frequencies, thereby drastically dropping the power output of the system. Since the system moves away from the resonant peak, it is no longer operating at the point where the impedance is minimum, as explained in 2.5, thus there will no longer be maximum current, thereby decreasing the power

output. This is primarily due to the fact that when the coupling factor changes, the reflected impedance from the receiving circuit to the transmitting circuit changes, thereby causing a shift in the behaviour of the class E amplifier system. There are few ways that the system can be tweaked, but the one that will be discussed here will be a frequency control method where the frequency of the system will be adjusted based on the coupling of the system.

Chapter 8

Conclusions and Future Works

The chapter consists of two sections, the conclusions that can be drawn from the work done in this paper, as well as a future works section which will discuss how the work can be furthered in the future.

8.1 Conclusions

The aim of this thesis report was to present a WPT system that would be capable of fully charging a 75 W drone within an hour. In order to do so, an amplifier circuit and coils had to be designed and tested through simulation. As presented in chapters2 and 4, both circuits discussed how the coils and the class E amplifier were designed and the results were presented there as well. Due to the COVID-19 restrictions preventing access to the lab, simulation testing account for all of the testing done on the circuits. From the results, it can be stated that the goal of the thesis was achieved as the circuit was able to deliver around 90 Watts of power to the battery of the drone. However, one would expect that the circuit would not perform as well in the real world as it does in simulation as there will be real world losses that cannot be accounted for with a simulation software such as LT Spice. It is not exactly sure how the coupling of the two coils will be in the real world, thus all of the simulations done and the circuit design assume that the system will have a coupling factor of 0.2, but that is also not a certainty. Furthermore, the components in the real world will not have ideal behaviour as they do in the simulations, thus the system will need to be tuned while it is being built and tested. However, through the sensitivity analysis, the general behaviour of the circuit to different parameter changes is known, therefore diagnosing issues with the circuit in the real world will be clearer.

The coils that were designed based on the inductance value provided from the amplifier circuit seemed to make sense and were realisable when taking the practical restrictions into account. The receiving coil has an outer diameter of 15 cm outer

diameter with 4 turns, which is reasonable size for a coil that must have an self inductance of 2.76 uH. The size of 15 cm also makes it viable to be placed on the drone without substantially reducing the payload capacity. Similarly, the outer diameter of transmitting coil is 30 cm which is also a reasonable size for a coil with a self inductance of 4 uH that is transmitting 95 Watts of power. Through this process, it was uncovered that a successful design process constantly requires development of predeveloped systems and requires refinement between all the relevant domains.

The class E amplifier circuit, worked well and was able to achieve zero voltage and current switching while supplying the necessary amount of power to charge the drone. There was a potential simulation error that did not paint the proper picture of the total efficiency of the system.

The receiver also performed as expected and with Silicon Carbide diodes, the losses on the diodes were reduced even further, and the system was operating at an even more efficient state. The value of the capacitor was modified to find the right compromise between start up time and voltage fluctuations. The design of the receiver circuit was straight forward and did not pose any unique challenges since it consisted only of passive components. However, after coupling the transmitting and the receiving, the transmitting circuit behaved differently, since the reflected impedance played a role in the transmitting circuit as well, leading to some parameter changes in the primary circuit.

Using the different models to understand the different behaviours of the circuit helped build understanding of how the entire system works as a whole. The use of the model broke down the system into smaller parts that could be analysed separately before putting them all together and seeing the total behaviour of the circuit in the complete system model.

The sensitivity analysis also helped in concluding that this WPT system is sensitive to change in the system, thus there must a control system put into place that will compensate certain parts of the circuit to bring the system back into resonant operation. Through this report, it was clear to see that the coupling factor has a very dramatic effect on the system and affects the resonant frequency. Similarly, a relationship between the coupling factor and the impedance was also observed as it could be seen how the change in the coupling factor of the system affect the reflected impedance and thereby also changed the resonance trough.

All in all, the overall system behaved as expected and all of the different subsystems in the circuit came together to form an entire system that was able to supply 95 Watts to the DJI F550 drone at a coupling factor of 0.2.

8.2 Future Works

There are multiple things that can be improved in this system in the future which will make the system more robust and also more viable in real world usage. First of all, the system can be improved by designing a control system that adjusts the necessary parameters according to the data measured from the circuit. As mentioned earlier, the reflected impedance could be measured to know how the resonant peak has moved, which can thereafter be corrected by a system that tunes the frequency of the system.

8.2.1 Frequency Control System

A frequency control system is one that tunes the operation frequency of the system based on the reflected impedance that is observed in the primary circuit. This method is discussed in detail in paper [20] where a control system measures the reflected impedance as it varies with the coupling factor, thereby adjusting the frequency. This is done while keeping the resonant capacitor values constant, thereby the resonant inductor values as well. In order to do this, first the reflected impedance of circuit is determined through the equations discussed in detail in [20], thereby prompting a calculation for the DC feed choke inductor as well as the shunt capacitor. The details of how this method is executed is laid out very thoroughly in [20], but the general idea is to initially measure the reflected impedance of the system, and thereafter tune the frequency, shunt capacitor and the DC choke inductor to ensure the optimum switching conditions of the amplifier and efficiency power transfer.

In order to make this tuning system viable during operation, the DC choke inductor must be adjusted electronically instead of mechanically, and this can be done using a saturable reactor, where the magnetic core can be saturated by applying an external DC current, resulting in the change of the inductive reactance of the inductor. By changing the permeability of the core, the inductance of the system can change. This entails that the DC choke inductor cannot be an air- core coil and must have a core in order to electronically control its inductance [21].

This is one way that the system could be controlled when the coupling factor or another factor changed in order to re-tune the system back into resonance.

8.2.2 Mechanical realignment system

Another solution that could be discussed to improve the overall performance of the system would a mechanical alignment system that would align both the coils regardless of where the drone lands in order to ensure the highest possible coupling

all the time. This could be done by moving the transmitting coil to make sure that it is perfectly under the receiving coil, thereby ensuring the maximum possible coupling. Implementing a misalignment system would solve the problem of the resonant frequency shifting and would use the reflected impedance calculated by the control system to realign the two coils in order to always operate at 13.56 MHz.

Bibliography

[1] "DJI - The World Leader in Camera Drones/Quadcopters for Aerial Photography." [Online]. Available: https://www.dji.com/nl/flame-wheel-arf/feature

[2] J. M. Miller, A. Ansari, D. B. Heinz, Y. Chen, I. B. Flader, D. D. Shin, L. G. Villanueva, and T. W. Kenny, "Effective quality factor tuning mechanisms in micromechanical resonators," p. 041307, 12 2018. [Online]. Available: https://aip.scitation.org/doi/abs/10.1063/1.5027850

[3] "Qi Coupling Factor — Wireless Power Consortium." [Online]. Available: https://www.wirelesspowerconsortium.com/knowledge-base/magnetic-induction-technology/how-it-works/coupling-factor.html

[4] V. Shevchenko, O. Husev, B. Pakhaliuk, O. Karlov, and I. Kondratenko, "Coil design for wireless power transfer with series-parallel compensation," *2019 IEEE 2nd Ukraine Conference on Electrical and Computer Engineering, UKRCON 2019 - Proceedings*, pp. 401–407, 2019.

[5] B. H. Waters, B. J. Mahoney, G. Lee, and J. R. Smith, "Optimal coil size ratios for wireless power transfer applications," *Proceedings - IEEE International Symposium on Circuits and Systems*, vol. 1, no. 1, pp. 2045–2048, 2014.

[6] C. H. Choi, H. J. Jang, S. G. Lim, H. C. Lim, S. H. Cho, and I. Gaponov, "Automatic wireless drone charging station creating essential environment for continuous drone operation," *2016 International Conference on Control, Automation and Information Sciences, ICCAIS 2016*, no. October 2016, pp. 132–136, 2017.

[7] A. Rohan, M. Rabah, M. Talha, and S.-H. Kim, "Development of Intelligent Drone Battery Charging System Based on Wireless Power Transmission Using Hill Climbing Algorithm," *Applied System Innovation*, vol. 1, no. 4, p. 44, 2018.

[8] A. B. Junaid, A. Konoiko, Y. Zweiri, M. N. Sahinkaya, and L. Seneviratne, "Autonomous wireless self-charging for multi-rotor unmanned aerial vehicles," *Energies*, vol. 10, no. 6, pp. 1–14, 2017.

[9] N. O. Sokal and A. D. Sokal, “Class E-A New Class of High-Efficiency Tuned Single-Ended Switching Power Amplifiers,” *IEEE Journal of Solid-State Circuits*, vol. 10, no. 3, pp. 168–176, 1975.

[10] “Series Resonance in a Series RLC Resonant Circuit.” [Online]. Available: https://www.electronics-tutorials.ws/accircuits/series-resonance.html

[11] B. N. O. Sokal, “Class-E RF Power Amplifiers,” pp. 9–20, 2001.

[12] “Schottky Diode or Schottky Barrier Semiconductor Diode.” [Online]. Available: https://www.electronics-tutorials.ws/diode/schottky-diode.html

[13] “Mutual Inductance of Two Adjacent Inductive Coils.” [Online]. Available: https://www.electronics-tutorials.ws/inductor/mutual-inductance.html

[14] “Quality Factor — Q Factor Formula — Electronics Notes.” [Online]. Available: https://www.electronics-notes.com/articles/basic_concepts/q-quality-factor/basics-tutorial-formula.php

[15] C. Nataraj, S. Khan, and M. H. Habaebi, “Coil geometry models for power loss analysis and hybrid inductive link for wireless power transfer applications,” *Sadhana - Academy Proceedings in Engineering Sciences*, vol. 43, no. 5, pp. 1–11, 2018. [Online]. Available: https://doi.org/10.1007/s12046-018-0842-x

[16] “American Wire Gauge Chart and AWG Electrical Current Load Limits table with ampacities, wire sizes, skin depth frequencies and wire breaking strength.” [Online]. Available: https://www.powerstream.com/Wire_Size.htm

[17] “Skin and Proximity Effects of AC Current - Technical Articles.” [Online]. Available: https://www.allaboutcircuits.com/technical-articles/skin-and-proximity-effects-of-ac-current/

[18] “S-Parameters for Antennas (S11, S12, ...).” [Online]. Available: http://www.antenna-theory.com/definitions/sparameters.php

[19] M. Chinthavali and Z. J. Wang, “Sensitivity analysis of a wireless power transfer (WPT) system for electric vehicle application,” *ECCE 2016 - IEEE Energy Conversion Congress and Exposition, Proceedings*, 2016.

[20] S. Aldhaher, P. C. K. Luk, and J. F. Whidborne, “Electronic tuning of misaligned coils in wireless power transfer systems,” *IEEE Transactions on Power Electronics*, vol. 29, no. 11, pp. 5975–5982, 2014.

[21] “What does reactor mean?” [Online]. Available: https://www.definitions.net/definition/reactor

Appendix A

MATLAB

A.1 Recieving Coil Code

```
Di = 0;
l=0;
a = 0;
c = 0;
L = 0;
C = 0;
Rdc = 0;
delta = 0;
R = 0;
Q = 0;

sig = 59.6*10^6;
delta = 0;
mu = 1.2566*10^-6;
D0 = 0.15;
w1= 0.00205232;
p1 = 2.8*w1
N1 = 4;
f = 13.56*10^6;
omega = 2*pi*f;

Di = D0 - 2*N*(w1+p)
l = (1/2)*N*pi*(D0+Di)
a = 0.25*(D0+Di)
```

```
c=0.5*(D0-Di)

L2 = ((N1^2*(D0-N1*(w1+p))^2)/(16*D0+28*N1*(w1+p)))*(39.37/10^6)
C2 = 0.85*(1/(((2*pi*f)^2)*L2))
Rdc = (l)/(sig*pi*(w/2)^2)
delta = (1)/(sqrt(pi*f*sig*mu))
R= Rdc*(w/(4*delta))
Q2 = (1/R)*(omega*L2)
n = 1- (2/(0.1*sqrt(Q1*Q2)))
q = Q1/Q2;
Q = sqrt(Q1*Q2);
g = 3/(omega*L2);
lambda = 1/(q*Q*g);
eff = 1/(1+lambda)
```

A.2 Transmitting Coil Code

```
%% Calculating Di
Di = 0;
l=0;
a = 0;
c = 0;
L = 1;
C = 0;
Rdc = 0;
delta = 0;
R = 0;
Q = 0;
Resit = 0;


sig = 59.6*10^6;
delta = 0;
mu = 1.2566*10^-6;
D0 = 0.3;
w= 0.00205232;
p = 9.1*w
N = 4;
f = 13.56*10^6;
```

```
omega = 2*pi*f;

Di = D0 - 2*N*(w+p)
l = (1/2)*N*pi*(D0+Di)
a = 0.25*(D0+Di)
c=0.5*(D0-Di)

L1 = ((N^2*(D0-N*(w+p))^2)/(16*D0+28*N*(w+p)))*(39.37/10^6)
C1 = 0.85*(1/(((2*pi*f)^2)*L1))
Rdc = (l)/(sig*pi*(w/2)^2)
delta = (1)/(sqrt(pi*f*sig*mu))
R= Rdc*(w/(4*delta))
Q1 = (1/R)*(omega*L1)
Resit= 0.00521*l
```

A.3 T-Model MATLAB Code

```
k = 0.2;
L1p = 4e-6;
L2p  = 2.76e-6;
Rloadopt = 3;
w = 2*pi*13.56e6
M = 0.2*(sqrt(L1p*L2p))
L1 = L1p - M
L2 = L2p - M
C1 = 0.85*(1/((13.56e6)^2*4*pi^2*L1p))
C2 = 0.85*(1/((13.56e6)^2*4*pi^2*L2p))
L2p = Rloadopt/ (w*k)
```

A.4 Class E Amplifier Code

```
%% Calculate Parameter Values
R_L=3;
fs=13.56e6;
Co = 750e-12;
C1 = 1000e-12;
L2 = 8.1872e-04;
Vin = 100;
```

```
C1 = 1/(2*pi*fs*R_L*5.447)
L1 = ((pi^2+4)*R_L)/fs
C2= 1/(((2*pi*fs)^2)*L2)
Ceq=((C1+Co)*C2)/(C1+Co+C2)
f1 =(1)/((2*pi)*(sqrt(L2*C2)))
f2 =(1)/((2*pi)*(sqrt(L2*Ceq)))
check = 1/(2*f1) + 1/(2*f2)
Check2 = 1/fs
VbrDss = 3.56*Vin + 0.2*Vin
L2new = R_L / ((2*pi*fs)*0.2)
```